Short Papers

Circuit Parameters for Single and Coupled Microstrip Lines by a Rigorous Full-Wave Space-Domain Analysis

NIELS FACHÉ AND DANIËL DE ZUTTER

Abstract—A rigorous full-wave analysis is applied to determine the dispersion characteristics and the impedance matrix of coplanar microstrip lines. It is shown that the impedance definition based on the propagating power and the longitudinal current is the most appropriate one. Examples are given for the single strip, for two coupled strips, either symmetric or asymmetric, and for a three-strip configuration. Some attention is also devoted to the current profiles associated with each eigenmode.

I. Introduction

Although in the past considerable attention was already devoted to the analysis of the dispersion characteristics and to the calculation of the characteristic impedance of both single and coupled microstrip line configurations, the dynamic behavior and accurate modeling of such structures have gained increasing importance due their presence in high-speed interconnections.

The single and coupled microstrip problems have been analyzed by several methods. We refer the reader to [1]–[7] for a review of various approaches and results. Important results were obtained through the spectral-domain approach. A comprehensive review of papers up to October 1985 can be found in [2].

In the original spectral-domain approach the boundary conditions on the strip were only satisfied in a single point at the center of the strip. In the more recent publications using the spectral-domain approach either a more accurate closed-form representation of the current or a representation of the current using a larger number of basis functions is introduced. In these cases the boundary conditions are imposed in some global sense. In the present paper the full-wave solution proposed in [6] is applied to the single and coplanar multistrip problem. In the latter case it is essential to include enough degrees of freedom in the representation of the current distribution. Both the transverse and the longitudinal current are discretized using the method of moments in such a way that the edge conditions are satisfied. The boundary conditions on the strip are no longer imposed in a global sense, as in the spectral-domain approach, but at a number of points equally spaced along the strip. By explicitly satisfying the boundary conditions in the end points of each strip, not only is the high-frequency behavior handled correctly, but the numerical results remain accurate in the low-frequency and static limit.

As a result of the space-domain field analysis the dispersion characteristics of the structures under study are found. In order to obtain a complete transmission line equivalent for those structures, their characteristic impedance(s) must be determined. This important issue has been extensively discussed in the literature [8]–[12]. In Section III we start from the general outline given in [11] and [12] to compare the different results for the characteristic impedance obtained when voltage–current, power–voltage, and power–current definitions are used.

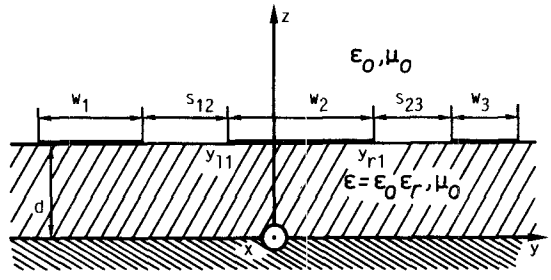

Fig. 1 Coupled microstrip lines on a dielectric substrate.

In Section IV, which constitutes the major part of this paper, we demonstrate the flexibility of our method by presenting numerical results for both the effective dielectric constant and the characteristic impedance(s) as a function of frequency for the single strip and for the coplanar coupled two-strip problem. Both symmetric and asymmetric coupled lines are considered. Results for the three-strip problem are also presented, demonstrating the flexibility of our method to be extended to many strips. In the coupled line cases the effective dielectric constant and the characteristic impedances must be supplemented by the ratio of the total longitudinal currents flowing along each strip to yield a complete equivalent network description of such structures [13]. Finally, special attention is also devoted to the numerical results for both the transverse and longitudinal currents on the strips.

II. General Formulation

The configuration under consideration consists of N coupled coplanar microstrips with variable width and gap spacing as shown in Fig. 1 for a three-strip configuration. The strips are infinitely thin and perfectly conducting. This is also the case for the ground plane at $z = 0$. The microstrip substrate (medium 1), with thickness d, consists of a lossless, nonmagnetic material with relative permittivity ϵ_r. The top layer is air (medium 2). The structure is assumed to be uniform and infinite in both the x and the z direction. For the calculation of the electromagnetic fields excited by one of the N lowest eigenmodes, we start from the surface current densities on each strip. To solve the field problem and to determine the eigenvalues and eigenmodes of the coupled strips, we start from a suitable integral equation. The electrical Green's dyadic for the layered structure constitutes the kernel of this integral equation. We refer the reader to [6] for the actual form of this integral equation and for its solution technique. The method in [6] is a combination of the method of moments and a point-matching technique. The basis functions used to represent the current are chosen in such a way that Meixner's edge conditions are explicitly satisfied in the end points of each strip.

Manuscript received January 6, 1988; revised July 22, 1988. This work was supported by a grant from the Institut tot Aanmoediging van het Wetenschappelijk Onderzoek in Nijverheid en Landbouw and by the National Fund for Scientific Research of Belgium.

The authors are with the Laboratory of Electromagnetism and Acoustics, University of Ghent, Sint-Pietersnieuwstraat 41, 9000 Ghent, Belgium

IEEE Log Number 8824981.

III. Circuit Description of Single and Coupled Microstrips

A. Single Strip

The purpose of the proposed electromagnetic analysis of single and coupled microstrips is to obtain an equivalent (coupled) transmission line model which represents an accurate circuit description of the structures under consideration. These transmission line models can then be used together with device models in circuit simulators to analyze more complex circuits.

For pure TEM structures the voltage V_t and the current I_t in the transmission line model have the meaning of a voltage and a current in a circuit. The characteristic impedance is unique. The three possible definitions for the impedance Z, i.e., the power–current definition $Z = 2P/|I_t|^2$, the power–voltage definition $Z = |V_t|^2/(2P^*)$, and the voltage–current definition $Z = V_t/I_t$, give the same result. P represents the complex power $I_t^* V_t/2$ flowing along the TEM structure and along the equivalent transmission line.

For non-TEM structures, such as the microstrip, the problem is more difficult. In a recent paper, Brews discussed the transmission line models for dispersive waveguides [11]. As a starting point, he required that both waveguide and equivalent transmission line should have the same propagation constant β and propagate the same complex power P. This equivalence only requires the phase of Z to be constant (zero in the case of a lossless waveguide). The voltage V_t and the current I_t of the equivalent line can always be replaced by αV_t and I_t/α^*, where α is an arbitrary complex constant. As in the TEM case the power propagated in the modeled waveguide remains $V_t I_t^*/2$, but the amplitude of the characteristic impedance $Z = |\alpha|^2 V_t/I_t$ is not constant. The "voltage" V_t and the "current" I_t are weighted averages of the transverse electric and magnetic fields. In contradistinction to TEM structures, a circuit interpretation of V_t and I_t is not always possible. However, it is very important to note that the required equivalence between waveguide and transmission line model ensures that the three possible definitions for the characteristic impedance give the same result. Hence, different equivalent transmission line models differ in the choice of the amplitude of Z. This degree of freedom, which enables us to choose the amplitude of V_t, I_t, or Z, can be used to choose the voltage or the current in such a way that one of them can be given a circuit interpretation [12]. In this way it becomes possible to obtain a transmission line model which can be interconnected with (TEM) models for drivers and loads.

In the case of a single microstrip if the current is selected as the independent variable, it can be chosen to be the total longitudinal current I. If the voltage is selected as an independent variable, it can be chosen to be the strip center voltage V_c (calculated along the axis of symmetry of the strip). For both of the above choices, either the voltage or the current has a circuit interpretation. The question of which model is the most appropriate as a circuit description is extensively treated in [9]–[12]. The general conclusion is that a transmission line model based on the longitudinal current is the most accurate one. This model has the most TEM-like character [9], as will be shown by the numerical results presented in this paper. Due to this fact and to the fact that the total longitudinal current I is a physical quantity which is conserved when the strip is connected to a load or to a driver, the power–current model is the most suitable one for modeling interconnections between microstrip lines and TEM structures such as loads and drivers.

To characterize the equivalent transmission line we need the propagation constant β of the eigenmode, the total longitudinal current, and the propagated power. The first two quantities follow directly from the solution of the integral equation. The propagated power P can be found as the integration over the cross section of the microstrip of Poynting's vector projected onto the longitudinal x direction. Once the power P and the total longitudinal current $I = I_t$ are calculated, the characteristic impedance and the voltage of the equivalent transmission line under consideration are given by

$$Z_{PI} = 2P/|I_t|^2 \quad \text{and} \quad V_a = Z_{PI} I_t. \tag{1}$$

In Section IV this transmission line model is compared with an equivalent model based on the power and the strip center voltage and with a model based on the strip center voltage and the current. The latter is not an equivalent model because it does not propagate the same power as the actual microstrip line except in the quasi-TEM limit. In spite of the restricted usefulness of the last two models, it remains interesting to compare them with the power–current model in order to show that they yield the same result in the quasi-TEM limit and to illustrate the fact that there is a difference between the strip center voltage V_c and the voltage V_a defined in (1), which is a weighted average over the cross section of the structure. For the numerical details the reader is referred to the example discussed in Section IV.

B. Coupled Strips

To extend the power–current equivalent model for a single microstrip to coupled microstrips we have to determine how the total propagating power associated with each eigenmode is divided over the strips. For pure TEM structures this follows directly from a knowledge of the currents flowing along each conductor and from the voltage differences between each pair of conductors. The numerical results given in this paper are based on the following distribution of the total power P over the N strips proposed by Jansen [1]:

$$P_i = \iint_S (\boldsymbol{E} \times \boldsymbol{H}_i) \cdot \boldsymbol{u}_x \, dS \tag{2}$$

where P_i is the power associated with strip i and the integration extends over the surface S of the cross section of the structure. $\boldsymbol{E}$ is the total electric field and $\boldsymbol{H}_i$ is the field excited by the current on strip i. Definition (2) satisfies two necessary conditions: it yields the correct value of the total power and it gives correct results when applied to TEM structures. The impedance associated with strip i is given by [1]

$$Z_i = \frac{\iint_S (\boldsymbol{E} \times \boldsymbol{H}_i) \cdot \boldsymbol{u}_x \, dS}{2I_i^2} = P_i/(2I_i^2) \tag{3}$$

where I_i indicates the total longitudinal current on strip i. To obtain an impedance matrix of a coupled strip configuration we still need the ratios of the longitudinal currents, together with the strip impedances, strip powers, and the propagation constant. These ratios follow directly from the solution of the eigenmode problem. Not all of these quantities are independent [13]. In the case of symmetric two-strip configurations the current ratios are automatically 1 for the even modes or -1 for the odd modes.

IV. Numerical Results

In this section we have selected several examples both for the single-strip and for the coupled-strip problem in order to demonstrate the flexibility and accuracy of our method. In each case

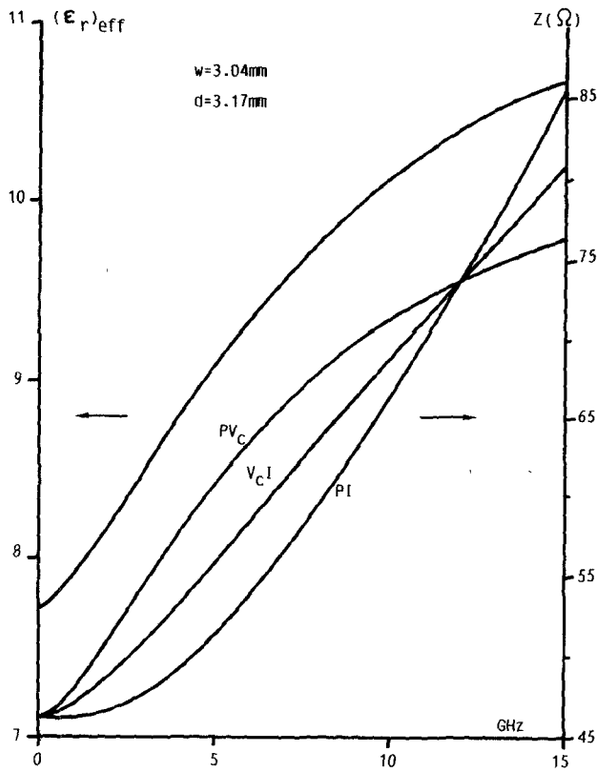

Fig. 2. Effective dielectric constant and impedances for a single strip ($w = 3.04$ mm, $d = 3.17$ mm, and $\epsilon_r = 11.7$).

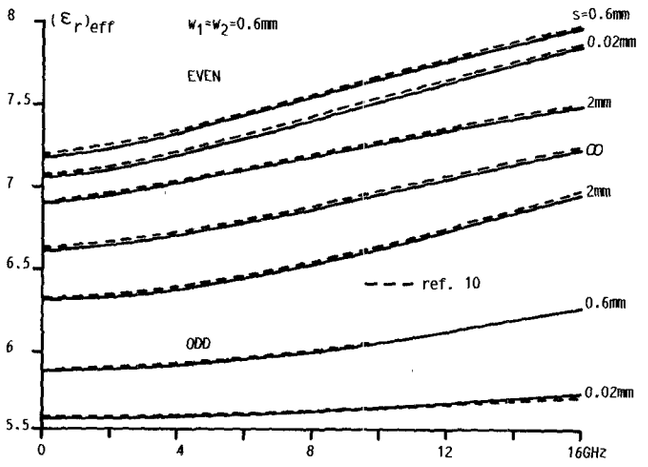

Fig. 3. Effective dielectric constant for two coupled strips with the gap spacing s as a parameter ($w_1 = w_2 = 0.6$ mm, $d = 0.64$ mm, and $\epsilon_r = 9.9$).

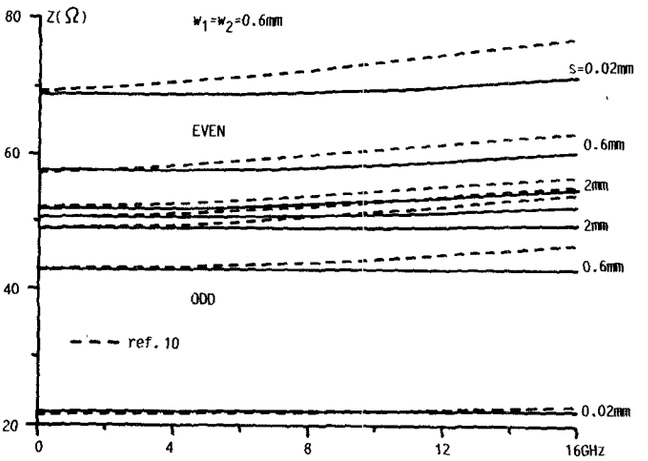

Fig. 4. Power-current impedance for two coupled strips with the gap spacing s as a parameter ($w_1 = w_2 = 0.6$ mm, $d = 0.64$ mm, and $\epsilon_r = 9.9$).

both the dispersion characteristic and the characteristic impedance(s) were calculated, leading to an equivalent transmission line representation for each eigenmode. To obtain converging results, no more than ten divisions per strip were needed for the dispersion characteristics and impedance results. For the current profiles, however, especially for the transversal currents, as many as 20 divisions turned out to be necessary.

Fig. 2 shows the effective dielectric constant $(\epsilon_r)_{\text{eff}} = (\beta/k_0)^2$ as a function of frequency $f = \omega/2\pi$ for a single strip of width $w = 3.04$ mm, substrate thickness $d = 3.17$ mm, and $\epsilon_r = 11.7$. Our results differ by less than 1 percent from the results in [3]. The other curves in Fig. 3 show the characteristic impedance calculated according to the three definitions given in Section III (PV_c: power–voltage; V_cI: voltage–current; PI: power–current). These results clearly illustrate the fact that the PI definition has the most TEM-like character [9] as its value only starts to increase at higher frequencies as compared with the PV_c and V_cI results. Analogous curves in [8], but for a different configuration, do not coincide in the low-frequency limit. As stated by the authors, this is due to inaccurate modeling of the currents. Our results clearly prove the accuracy of the current modeling proposed in this paper.

We now turn to some examples for the two-strip configuration. The full lines in Figs. 3 and 4 give the results of our approach for a typical symmetric coupled-strip configuration: width of each strip $w_1 = w_2 = 0.6$ mm, substrate thickness $d = 0.64$ mm, and $\epsilon_r = 9.9$. Fig. 3 shows the dispersion characteristics while Fig. 4 gives the characteristic impedances for both the even and the odd mode. The gap spacing s takes the values 0.02 mm, 0.6 mm, and 2 mm. The case $s = \infty$, which is the single-strip case, forms the boundary between even and odd modes. We have compared our results with the ones in [4] given in dashed lines. The results for $(\epsilon_r)_{\text{eff}}$ differ only slightly while the impedances differ considerably at higher frequencies. This is due to the fact that in [4] the PV_c definition is used, whereas the PI definition is used here. Looking at the full lines in Fig. 4, it becomes very clear that the impedances calculated through the PI definition (full lines) keep their static value over a considerably higher frequency range.

As a next example we discuss the asymmetric coupled-line problem also treated by Tripathi [7] starting from a parallel-plate waveguide analysis. The widths of the strips are $w_1 = 0.6$ mm and $w_2 = 0.3$ mm, the gap spacing $s = 0.4$ mm, the substrate thickness $d = 0.635$ mm, and $\epsilon_r = 9.7$. The longitudinal current J_x and the transversal current J_y at 1 GHz are shown in Figs. 5 and 6, for both the c mode and the π mode. J_x and J_y are in quadrature and the transversal current is four orders of magnitude smaller than the longitudinal one. The notation $\pi*(-1)$ in Fig. 5 and $c*(-1)$ in Fig. 6 indicates that the actual currents are found by reversing the sign of the results shown in the figure. Taking a close look at Fig. 5 shows that the amplitude of J_x for the c mode (full lines) is smaller near the neighboring edges of strip 1 and strip 2 as compared to the value at the other edges. This is due to the repulsion between the currents for this mode.

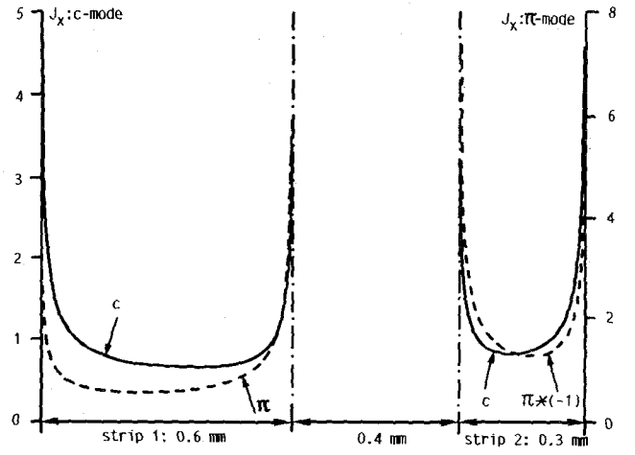

Fig. 5. Longitudinal current J_x at 1 GHz for an asymmetric strip configuration (c and π modes) with $w_1 = 0.6$ mm, $w_2 = 0.3$ mm, $s = 0.4$ mm, $d = 0.635$ mm, and $\epsilon_r = 9.7$.

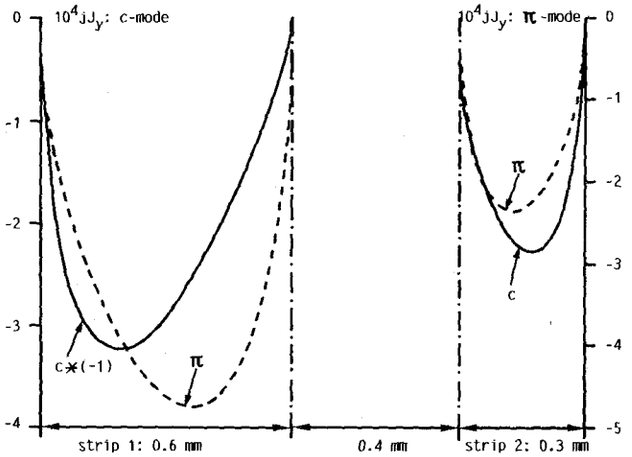

Fig. 6. Transversal current J_y at 1 GHz for the same configuration as in Fig. 5.

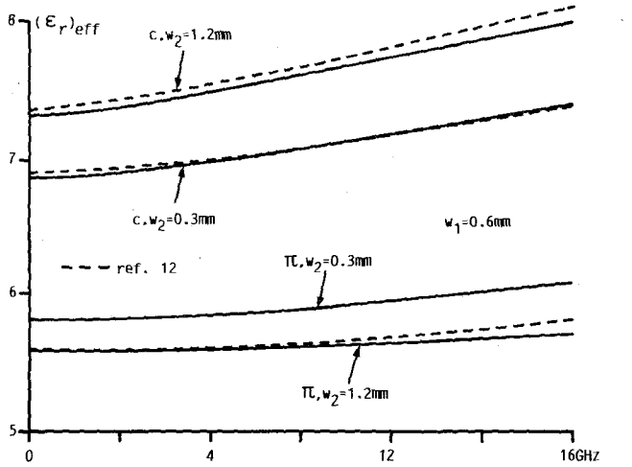

Fig. 7. Effective dielectric constant for the asymmetric coupled strip configuration of Fig. 5 and for a similar configuration with $w_2 = 1.2$ mm.

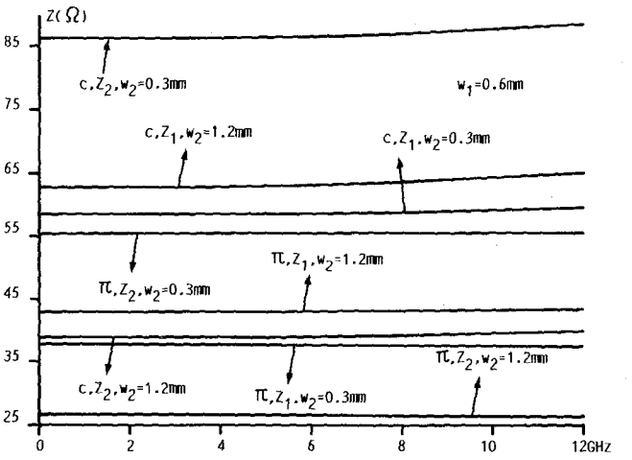

Fig. 8. Power–current impedances for the asymmetric coupled strip configuration of Fig. 7 and for a similar configuration with $w_2 = 1.2$ mm.

The situation is the other way around for the π mode (dashed lines).

The full lines in Fig. 7 give $(\epsilon_r)_{\text{eff}}$ as a function of frequency for the asymmetric configuration discussed above and for a similar configuration but with $w_2 = 1.2$ mm instead of $w_2 = 0.3$ mm. The dashed lines are the corresponding results from [7]. For the π mode and for $w_2 = 0.3$ mm, both results coincide. Fig. 8 shows the impedances associated with each strip as defined by (3) for the same parameters as in Fig. 7. In this case no corresponding results can be found in [7]. It is again clear that the impedances differ only slightly from their static values. As explained in Section III, the circuit description must be supplemented with the ratios of the total longitudinal currents. As these ratios change only very slightly over the selected frequency range we restrict our results to 1 GHz. At this frequency and for $w_2 = 0.3$ mm the ratio of the total longitudinal currents I_2 on strip 2 to the total current I_1 on strip 1 for the c mode is $I_2/I_1 = 0.647$ and $I_2/I_1 = -1.046$ for the π mode. For $w_2 = 1.2$ mm this becomes $I_2/I_1 = 1.762$ for the c mode and $I_2/I_1 = -0.923$ for the π mode.

Finally, in order to show the applicability of our method to the multistrip problem, we turn to the strip configuration of Fig. 9. The three strips have equal widths $w_1 = w_2 = w_3 = 1$ mm and equal gap spacings $s_{12} = s_{23} = 1$ mm. The substrate thickness $d = 1$ mm and $\epsilon_r = 10$. For the currents we have restricted the results to the longitudinal J_x current at 1 GHz for the first and second even mode and for the first odd mode, as shown on Fig. 9. The solid lines in Fig. 10 give the effective dielectric constant as a function of frequency for these three modes. The dashed lines show the impedances. For each mode $Z_1 = Z_3$ and for the odd mode the total longitudinal current on strip 2 and the associated power (2) are zero; hence Z_2 is not defined and in fact is not needed in the equivalent transmission line representation. Two other dash–dot curves are shown in Fig. 10. They give the ratio $|I_2/I_1|$ of the total longitudinal current I_2 of strip 2 and the corresponding current $I_1 = I_3$ on strip 1 for the first and second even mode. For the odd mode this ratio vanishes as $I_2 = 0$.

V. Conclusion

Based on a full-wave analysis of the eigenmodes of coupled coplanar strips we obtained an equivalent transmission line representation for these structures by determining their dispersion characteristics and their impedance matrix as well as the ratios of the total longitudinal currents flowing on each strip.

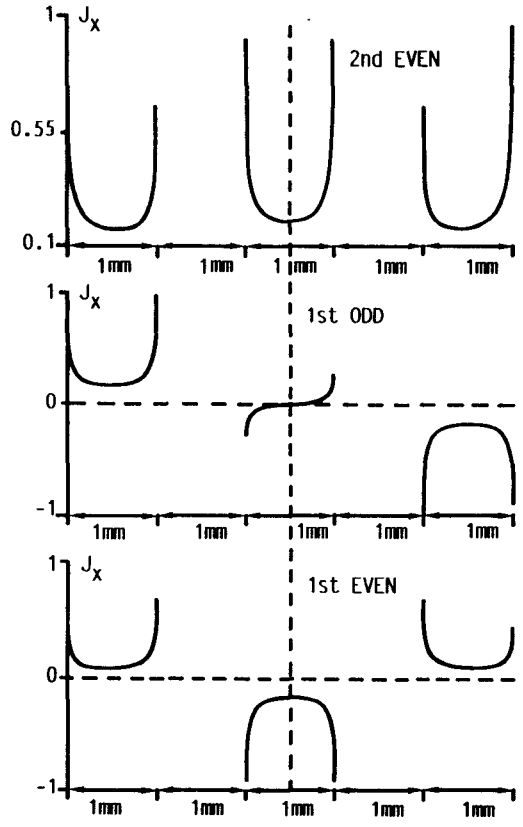

Fig. 9. Longitudinal current J_x at 1 GHz for a three-strip problem with $w_1 = w_2 = w_3 = 1$ mm, $s_{12} = s_{23} = 1$ mm, $d = 1$ mm, and $\epsilon_r = 10$.

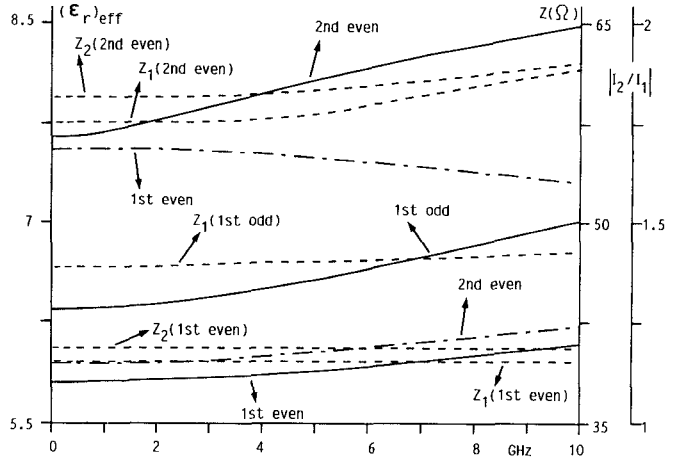

Fig. 10. Dispersion characteristics, power–current impedances, and total longitudinal current ratios for the three-strip configuration of Fig. 9.

For the single-strip configuration we compared the voltage–current, power–voltage, and power–current definitions for the characteristic impedance. It was shown that the power–current definition has the most TEM-like character, as it changes more slowly as a function of frequency than the other definitions. This property also holds good for the double- and triple-strip configurations, as was shown by some typical examples.

By incorporating Meixner's edge conditions and by explicitly satisfying the relevant integral equation in the end points, an accurate solution is ensured for all field quantities in both the low-frequency and the high-frequency range.

References

[1] R. H. Jansen, "Unified user-oriented computation of shielded, covered and open planar microwave and millimeter-wave transmission-line characteristics," *Microwaves, Optics and Acoustics*, vol. 3, pp. 14–22, Jan. 1979.

[2] R. H Jansen, "The spectral domain approach for microwave integrated circuits," *IEEE Trans. Microwave Theory Tech.*, vol. MTT-33, pp. 1043–1056, Oct. 1985.

[3] M. Kobayashi and F. Ando, "Dispersion characteristics of open microstrip lines," *IEEE Trans. Microwave Theory Tech.*, vol. MTT-35, pp. 101–105, Feb. 1987.

[4] R. H Jansen, "High-speed computation of single and coupled microstrip parameters including dispersion, higher-order modes, loss and finite strip thickness," *IEEE Trans. Microwave Theory Tech.*, vol. MTT-26, pp. 75–82, Feb. 1978.

[5] Y. Fukuoka, Q. Zhang, D. Neikirk, and T. Itoh, "Analysis of multilayer interconnection lines for a high-speed digital integrated circuit," *IEEE Trans. Microwave Theory Tech.*, vol. MTT-33, pp 527–532, June 1985.

[6] N. Faché and D. De Zutter, "Rigorous full wave space domain solution for dispersive microstrip lines," *IEEE Trans. Microwave Theory Tech.*, vol. MTT-36, pp. 732–737, Apr. 1988.

[7] V. K. Tripathi, "A dispersion model for coupled microstrips," *IEEE Trans. Microwave Theory Tech.*, vol. MTT-34, pp. 66–71, Jan. 1986.

[8] J. B. Knorr and A. Tufekcioglu, "Spectral-domain calculations of microstrip characteristic impedance," *IEEE Trans. Microwave Theory Tech*, vol. MTT-23, pp. 725–728, Sept. 1975.

[9] R. H. Jansen and M. Kirschning, "Arguments and an accurate model for the power-current formulation of microstrip characteristic impedance," *AEÜ*, band 37, heft 3/4, pp. 108–112, 1983.

[10] W J. Getsinger, "Measurement and modeling of the apparent characteristic impedance of microstrip," *IEEE Trans. Microwave Theory Tech.*, vol. MTT-31, pp. 624–632, Aug. 1983.

[11] J. R. Brews, "Transmission line models for lossy waveguide interconnections in VLSI," *IEEE Trans. Electron Devices*, vol. ED-33, pp. 1356–1365, Sept. 1986.

[12] J. R. Brews, "Characteristic impedance of microstrip lines," *IEEE Trans. Microwave Theory Tech.*, vol. MTT-35, pp. 30–34, Jan. 1987.

[13] V. K. Tripathi, "On the analysis of symmetrical three line microstrip circuits," *IEEE Trans. Microwave Theory Tech.*, vol. MTT-25, pp. 726–729, Aug. 1978

A FET Amplifier in Finline Technique

JEAN L'ECUYER, MEMBER, IEEE,
GREGORY B. GAJDA, MEMBER, IEEE, AND
WOLFGANG J. R. HOEFER, SENIOR MEMBER, IEEE

***Abstract*—The successful design and realization of a stable FET amplifier in finline technique are presented. The circuit has been realized in integrated E-plane technology and features an input and an output port in unilateral finline and a combined microstrip/coplanar bias circuit. The amplifier has been designed for 17 GHz operation and has a gain of 6 dB over a bandwidth of 1 GHz using a NE67300 FET.**

I. Introduction

In this paper, the design and performance of a novel finline amplifier will be described. The essential features of this amplifier were briefly outlined in [1]. Very little work had been reported previously on the realization of field-effect transistor

Manuscript received January 12, 1988; revised July 27, 1988.

J. L'Ecuyer was with the Communications Research Centre, Department of communications, Ottawa, Canada. He is now with Spar Aerospace Ltd., 21025 Trans-Canada Highway, Ste-Anne-de-Bellevue, Quebec, Canada H9X 3R2.

G. B. Gajda was with the Communications Research Centre, Department of Communications, Ottawa, Canada. He is now with the Millennium Microwave Corporation, 380 Lewis St., Ottawa, Ont., Canada K2P 0S9.

W. J. R. Hoefer is with the Department of Electrical Engineering, University of Ottawa, Ottawa, Ont., Canada K1N 6N5.

IEEE Log Number 8824985.